UC Berkeley

Title

Myocardial blood flow measurement with a conventional dual-head SPECT/CT with spatiotemporal iterative reconstructions – a clinical feasibility study.

Permalink

https://escholarship.org/uc/item/1fg7m5d4

Journal

Am j nucl med mol imaging, 4(1)

ISSN

2160-8407

Authors

Alhassen, Fares
Nguyen, Nhan
Bains, Sukhkarn
et al.

Publication Date

2014

Peer reviewed

Original Article
Myocardial blood flow measurement with a conventional dual-head SPECT/CT with spatiotemporal iterative reconstructions - a clinical feasibility study

Fares Alhassen[1], Nhan Nguyen[1,2], Sukhkarn Bains[1], Robert G Gould[1], Youngho Seo[1], Stephen L Bacharach[1], Xiyun Song[3], Lingxiong Shao[3], Grant T Gullberg[1,4], Carina Mari Aparici[1,4]

[1]Center for Molecular and Functional Imaging, Department of Radiology and Biomedical Imaging, University of California, San Francisco, CA, USA; [2]Nuclear Medicine Service, San Francisco Veterans Affairs Medical Center, San Francisco, CA, USA; [3]Philips Healthcare, San Jose, CA, USA; [4]Department of Radiotracer Development & Imaging Technology, Lawrence Berkeley National Laboratory, Berkeley, CA, USA

Abstract: Cardiac single photon emission computed tomography (SPECT) cameras typically rotate too slowly around a patient to capture changes in the blood pool activity distribution and provide accurate kinetic parameters. A spatiotemporal iterative reconstruction method to overcome these limitations was investigated. Dynamic rest/stress ^{99m}Tc-methoxyisobutylisonitrile (^{99m}Tc-MIBI) SPECT/CT was performed along with reference standard rest/stress dynamic positron emission tomography (PET/CT) ^{13}N-NH$_3$ in five patients. The SPECT data were reconstructed using conventional and spatiotemporal iterative reconstruction methods. The spatiotemporal reconstruction yielded improved image quality, defined here as a statistically significant ($p<0.01$) 50% contrast enhancement. We did not observe a statistically significant difference between the correlations of the conventional and spatiotemporal SPECT myocardial uptake K_1 values with PET K_1 values (r=0.25, 0.88, respectively) ($p<0.17$). These results indicate the clinical feasibility of quantitative, dynamic SPECT/CT using ^{99m}Tc-MIBI and warrant further investigation. Spatiotemporal reconstruction clearly provides an advantage over a conventional reconstruction in computing K_1.

Keywords: Dynamic SPECT, myocardial perfusion imaging, ^{99m}Tc-MIBI, SPECT/CT, spatiotemporal reconstruction, uptake rate constant

Introduction

Quantitative, dynamic myocardial perfusion imaging (MPI) in positron emission tomography (PET) using tracers such as ^{15}O-H$_2$O, ^{13}N-NH$_3$, and ^{82}Rb yields kinetic parameters such as myocardial blood flow and flow reserve that provide additional technical and clinical information not available from static MPI acquisitions [1-4]. Single photon emission computed tomography (SPECT) is the clinical workhorse for MPI but is not clinically used to obtain absolute kinetic parameters [5]. In dynamic acquisitions, the slowly rotating cameras typical of SPECT scanners yield inconsistent projections.

Nevertheless, there have been a few studies of kinetic parameter estimation using dynamic SPECT. For example, quantification of regional myocardial blood flow using a nonstress proto-

col has been performed, with validation using ^{13}N-NH$_3$ PET [6]. Preliminary work comparing kinetic parameters obtained from spatiotemporal-reconstructed, PET-derived, SPECT data has also shown that the 1 min acquisition times typical of clinical SPECT scanners may be sufficient for quantitatively accurate kinetic parameter estimation [7]. These initial results and our current efforts of estimating kinetic parameters such as myocardial blood flow using dynamic SPECT all indicate that there could be a significant economic advantage over the same parameter estimation using dynamic PET [8].

Here, we performed a clinical study of five patients using a dynamic rest/stress ^{99m}Tc-MIBI SPECT protocol and a clinical, dynamic, rest/stress ^{13}N-NH$_3$ PET protocol. We reconstructed the SPECT data using a commercial maximum-likelihood expectation-maximization (MLEM)

reconstruction software package and a spatio-temporal MLEM (ST-MLEM) reconstruction [7].

Materials and methods

Patient population

Five patients were recruited at the San Francisco VA Medical Center (San Francisco, CA) to test a new dynamic SPECT MPI protocol. In addition, the patients underwent clinical PET MPI studies at the University of California San Francisco Outpatient Imaging Center at China Basin (San Francisco, CA). The study was approved by the VA Medical Center Committee on Human Research as well as the University of California, San Francisco, Committee on Human Research (Institutional Review Board). The patients were considered for study if a myocardial perfusion study had been requested by their clinician. The recruited patients gave written consent to be part of the study. The patients had risk factors but no prior history of coronary artery disease (CAD).

Dynamic and clinical SPECT acquisition protocol

The rest/stress MPI acquisition, following a low-/high-activity single isotope single-day protocol was performed using a SPECT/CT scanner (Precedence 16, Philips Healthcare). The scanner has two L-configured (i.e., oriented 90° to each other) detector heads, each with a low-energy high-resolution (LEHR) collimator. Projection data were binned into 128×128 matrix having 3.2×3.2 mm^2 pixels, over 36 projection angles spanning 0-180°.

The patients were instructed to fast for 4 hours and to not smoke or consume anything with caffeine or xantines 24 hours prior to the test. None of the subjects was taking beta-blockers, statins or nitrates. The imaging protocol began with a dynamic rest image acquisition. Imaging began just prior to activity infusion, with patients lying in supine positions. The dynamic image acquisition consisted of twelve back-and-forth rotations, with each 180° rotation (90° per head) taking 54 seconds to acquire (total ~ 12 min). Once the scanner heads began rotating, each patient received continuous two-minute infusions of approximately 370 MBq (10 mCi) of ^{99m}Tc-MIBI (Cardiolite; Bristol-Myers Squibb Medical Imaging) using a Harvard Apparatus Model 975 pump, with a typical ±20% variation in activity between patients. The patients then waited 45 minutes before a

clinical, non-dynamic, rest SPECT/CT scan was performed, consisting of a single 180° rotation over 25 minutes. A CT scan for attenuation correction (AC) was acquired just before the clinical scan. Fifteen minutes after the completion of the rest clinical scan, and with the patient still in the scanner, the patients underwent an equivalent stress dynamic/clinical SPECT MPI acquisition, with a 0.4 mg bolus injection of a regadenoson stress agent (Lexiscan; Astellas Pharma, Inc.) followed by a ^{99m}Tc-MIBI activity of 1150 MBq again using a 2 minute infusion. Data acquisition started when activity was observed in real-time moving from the arm to the subclavian vein in the scanner field-of-view for both rest and stress studies. Another CT scan for AC was performed just before the clinical, non-dynamic, stress scan. Although the whole rest-stress SPECT MPI scans including our research dynamic SPECT sessions took at least 2.5 hours or more, it should be noted that even a clinical SPECT MPI protocol alone can consume a long time when both rest and stress scans are acquired on the same day. In addition, when the soft tissue attenuation is suspected or the patient requires a prone positioning, the scan time could be even longer [8-10].

PET acquisition and image reconstruction protocol

The SPECT patient cohort also had ^{13}N-NH$_3$ PET/CT MPI scans performed within 1 to 17 days using a PET/CT scanner (Discovery VCT, GE Healthcare) following a standard clinical protocol based on ASNC guidelines [11]. None of the patients in the cohort experienced a cardiac event in between the two scans. A 12.5-minute dynamic rest scan was performed with a 740 MBq ^{13}N-NH$_3$ bolus injection, followed by a 45 minute break, and then a pharmacologic stress scan with ^{13}N-NH$_3$ using the same stress agent administration (regadenoson) as with the stress SPECT scans. Each of the 25 dynamic frames of the PET data was reconstructed using 2D filtered back-projection (FBP) with a Hanning window and a 4.8 mm convolution kernel. Data were corrected for attenuation and randoms.

Conventional and spatiotemporal iterative reconstruction

The dynamic SPECT data from each rotation were reconstructed using the Philips Astonish ordered-subsets-expectation-maximization-based (OS-EM) reconstruction software pack-

age, yielding a set of twelve 2D image sets per dynamic scan with dimensions $128 \times 128 \times N_z$, where N_z was the patient-dependent number of reconstructed slices. A total of 54 MLEM iterations (i.e., 1 OS-EM subset) were used per reconstruction with AC. Attenuation maps for the AC reconstruction were generated by co-registering the acquired CT data using the Philips JetStream Workstation.

The same projection data were also reconstructed using a ST-MLEM reconstruction software package developed by Lawrence Berkeley National Laboratory (LBNL) [7]. The LBNL reconstruction used an MLEM algorithm with AC to iteratively reconstruct the coefficients of a set of quadratic B-spline basis functions per voxel. The ST-MLEM-reconstructed basis function coefficients were converted into time-activity data, with the basis functions sampled at an approximately three times higher rate than the 12 time points from the ST-MLEM reconstruction, yielding 37 time points. The midpoints of each temporal frame were selected for the time points for the time-activity data (e.g., 27 s for a 54 s frame). Since we reconstructed a total of 37 time points (i.e., 37 frames of dynamic SPECT), the increased reconstruction time was proportional to the number of dynamic frames required for our data analysis.

No depth-dependent resolution recovery or partial volume correction was performed for either the MLEM or ST-MLEM reconstruction. The reconstructed SPECT data were 3D Gaussian-filtered ($9 \times 9 \times 9$ voxel kernel, 6.4 mm full-width half-maximum (FWHM)) in MATLAB for basic image quality evaluation. The filter parameters were chosen to yield images comparable to those obtained using GE Myovation software using a Butterworth filter with a cutoff frequency of 0.4 cm^{-1}, an order of 5, an 16×16 voxel kernel, based on vendor recommended settings.

Time-activity curves (TACs) of tissue and input function were generated by calculating average activity values in left myocardial and blood pool ROIs. The left atrium was chosen to represent the blood pool [12]. ROIs were first drawn on the filtered PET data and then copied and manually registered to the SPECT data.

Data analysis

The uptake rate constant (K_1) for ^{99m}Tc-MIBI SPECT was each computed using a one-tissue-compartment model

$$C_t(t) = [K_1 \exp(-k_2 t) \otimes (1-f_s)C_a(t)] + f_s C_a(t) + C_0 \quad (1)$$

Where $C_t(t)$ was the modeled myocardial tissue TAC, $C_a(t)$ the input left atrial TAC, k_2 the myocardial washout coefficient, f_s the fraction of blood of the input activity in the tissue compartment, and $\otimes$ denotes the one-dimensional convolution operation [3]. C_0 is the leftover rest activity visible in stress data and was set to zero for rest data. The unknown parameters K_1, k_2, f_s, and C_0 were determined by fitting the first five minutes of the PET and SPECT TACs to **Equation 1** using the interior point nonlinear optimization method available in Mathematica (Wolfram Research, Inc.) subject to the following constraints: all parameters were assumed to be greater than zero and the maximum value of f_s was 0.50, a constraint well above typical the 0.17-0.20 spillover fractions described elsewhere for ^{99m}Tc-MIBI [6]. The tracer distribution volume was assumed to be one. We also used the same one-tissue-compartment model for the K_1 calculations for ^{13}N-NH$_3$ PET.

Six out of the ten scans (i.e., rest scans from patients 1, 2, and 4, and stress scans from patients 1, 4, and 5) were used for kinetic analysis, as four of the acquisitions had started late, resulting in missing blood pool TAC data. The criterion for selecting data sets included for kinetic analysis was that the MLEM-reconstructed blood pool TAC should have not reached 75% of the peak blood pool value by $t = 27$ s (the first rotation).

Contrast scores were determined by calculating the ratio between the average values of the left myocardial and blood pool/left atrial ROIs for SPECT during the last two rotations (108 s total) for the SPECT data and during the last 300 s duration for the PET data. The scores were used as a metric for image quality. PET contrast was similarly calculated using the final PET frame (600 to 900 seconds).

MLEM TACs were normalized so that the peak blood pool activity was set equal to unity. The ST-MLEM TACs were then scaled so that the mean value of the activity in the last 216 s of the left myocardial curve was equal to that of the normalized MLEM TAC, respectively for rest and stress.

Statistical analyses

An unpaired *t*-test assuming unequal variance was used to determine statistically significant
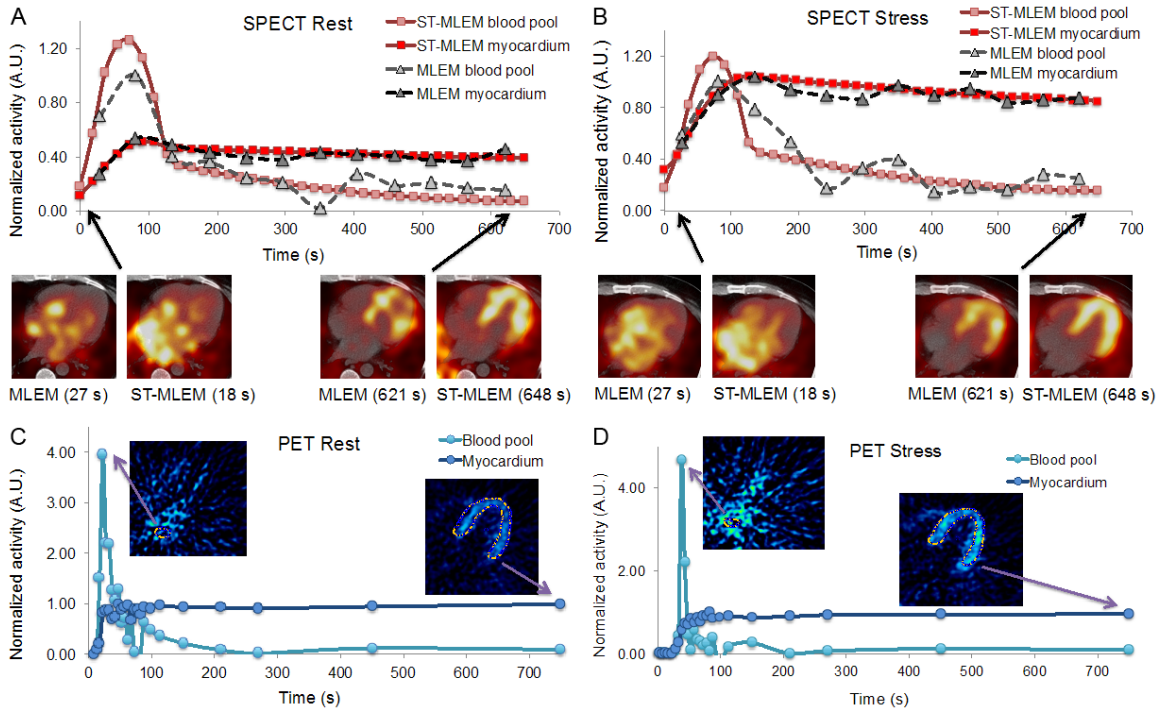
Figure 1. Five-minute TACs obtained using MLEM (gray) and ST-MLEM (red) SPECT reconstructions, along with transverse cross-sections of the left myocardium, of A rest, B stress data, and ^{13}N-NH$_3$ PET C rest and D stress data, all from the same patient. The blood pool/left atrial and left myocardial ROIs are shown in C and D.

Table 1. Contrast Scores

Data Set	PET	MLEM SPECT	ST-MLEM SPECT
Patient 1 - Rest	10.8	2.6	5.1
Patient 2 - Rest	11.3	2.7	4.3
Patient 3 - Rest	2.9	1.5	2.8
Patient 4 - Rest	3.9	1.6	3.3
Patient 5 - Rest	5.6	1.8	4.4
Patient 1 - Stress	10.1	3.3	5.4
Patient 2 - Stress	11.7	3.8	3.3
Patient 3 - Stress	8.3	5.0	4.2
Patient 4 - Stress	4.9	2.7	5.6
Patient 5 - Stress	9.5	2.8	3.4

differences between the SPECT and PET contrast scores. Pearson's linear correlation coefficient was used to determine the correlation between the PET and SPECT myocardial uptake coefficients. The significance of the difference between correlation coefficients was calculated using the Fisher r-to-z transformation. Unpaired Bland-Altman plots were used to check systematic or bias errors in the SPECT myocardial uptake coefficients with respect to the reference standard PET data. A two-tailed p-value less than 0.05 was considered to be statistically significant.

Results

MLEM vs. ST-MLEM SPECT time activity curves and transaxial myocardial images

Figure 1 shows blood pool and left myocardial TACs from a typical patient obtained using the SPECT reconstructions, along with transverse cross-sectional views of the left myocardium. The left myocardial curve was equal to that of the normalized MLEM TAC, respectively for rest and stress. Dynamic PET data for the same patient as in **Figure 1A** and **1B** are shown in **Figure 1C** and **1D**.

Comparing contrast scores

Table 1 contains the contrast scores for all data sets. **Figure 2A** shows the mean contrast scores for the five rest and five stress scans, with the error bars representing a single standard deviation (SD). **Figure 2B** contains late-time SPECT images illustrating typical differences in contrast between rest and stress and between MLEM and ST-MLEM reconstructions. In both rest and stress, the PET data had the highest contrast, followed by ST-MLEM SPECT and then MLEM SPECT. In the rest studies,
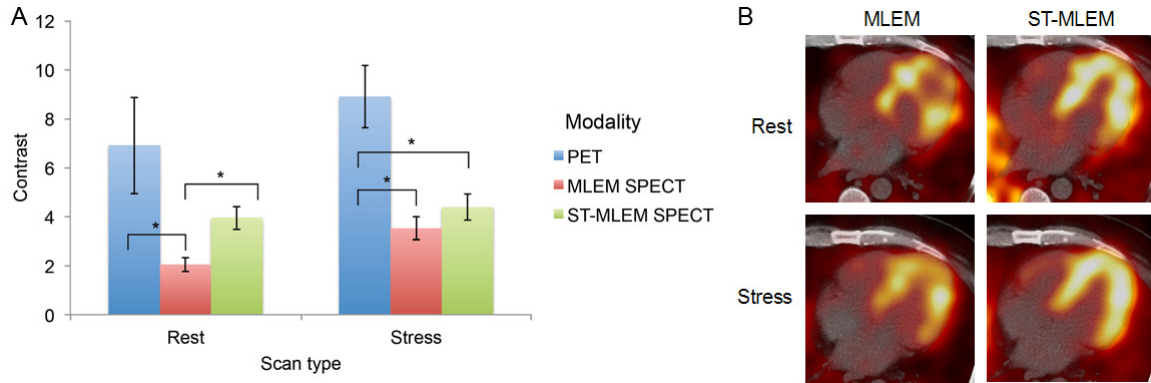
Figure 2. A: Contrast scores for PET, MLEM SPECT, and ST-MLEM SPECT data, at rest and stress. An asterisk (*) indicates a statistically significant difference ($p<0.05$) between the data sets. B: Late-time rest and stress SPECT images using MLEM and ST-MLEM reconstructions.
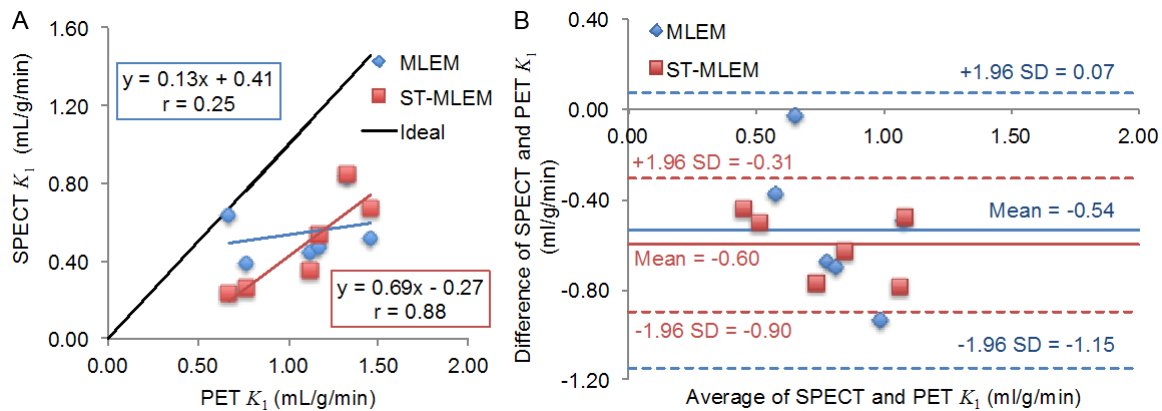

Figure 3. A: Correlations between SPECT and PET K_1 values, with r equal to 0.25 and 0.88 for the MLEM and ST-MLEM SPECT data, respectively, and B: Bland-Altman plot of the SPECT K_1 data using the PET K_1 values as the reference standard.

ST-MLEM SPECT yielded a statistically significant 50% increase in contrast over MLEM SPECT ($p<0.01$). There was no statistically significant difference between the PET and ST-MLEM SPECT data ($p<0.178$) while for the PET and MLEM SPECT data, there was a statistically significant difference ($p<0.05$). At stress, there was no statistically significant difference between the MLEM and ST-MLEM SPECT contrast ($p<0.21$). Both stress SPECT data sets had lower contrast than PET ($p<0.01$).

Myocardial uptake parameters

We compared the reference standard PET K_1 values with those computed from the MLEM SPECT and ST-MLEM SPECT (**Figure 3**). The correlation coefficient, r, with respect to the PET K_1 data was 0.25 for the MLEM SPECT data and 0.88 for ST-MLEM SPECT. There was no statisti-

cally significant difference between the correlation coefficients ($p<0.17$). Both SPECT K_1 sets exhibited similar negative biases with respect to PET K_1, -0.54 and -0.60 for MLEM and ST-MLEM SPECT, respectively (**Figure 3B**). The MLEM SPECT data had a slightly larger variation in the Bland-Altman plot than the ST-MLEM SPECT data (**Figure 3B**), and a larger 95% confidence interval (0.61 versus 0.30, respectively).

Discussion

The ST-MLEM reconstruction appears to improve the late-time image quality (> 120 s) for rest SPECT images, as the left myocardium appears less noisy and the contrast scores are higher than those obtained using the MLEM reconstruction. This is to be expected, as the ST-MLEM algorithm is able to use statistics

from all rotations and weight the contributions using linear sums of basis functions while the MLEM reconstruction only uses projections from a single rotation. Another effect is the smoothing of the frame-to-frame variations in the TACs.

However, one possible advantage of the ST-MLEM reconstruction over MLEM for stress data is that the ST-MLEM TACs were weighted sums of continuous functions and thus can naturally be sampled at $t = 0$ s. Thus, the left-over rest activity at the beginning of the stress scan can be determined from the iterative estimate of the background activity of the entire projection data set. The ST-MLEM therefore can automatically compensate for any residual activity (e.g. activity at stress from a previous rest study), without any explicit image subtraction. This feature of ST-MLEM may allow a more optimum rest/stress protocol - one which avoids the necessity of a low-high-activity regimen. This feature has yet to be thoroughly tested.

The correlations between the SPECT and PET K_1 values are limited by the fact that ^{99m}Tc-MIBI and ^{13}N-NH$_3$ PET are different tracers and thus have different pharmacokinetics (e.g. MIBI has much lower extraction than NH$_3$). Nevertheless, the MLEM and ST-MLEM TACs yielded statistically indistinguishable, although different, K_1 correlations with the PET K_1 data. A larger patient cohort would be needed to determine if there were any real differences in correlation. The slope of the correlation for the MLEM data was 0.25, similar to values of 0.20-0.30 observed in similar studies comparing myocardial flow obtained using ^{99m}Tc-MIBI scintigraphy with ^{15}O-H$_2$O PET and with ^{13}N-NH$_3$ PET [6, 13]. In comparison, ST-MLEM yielded a higher slope of 0.69, while still having a similar bias of ~ -0.60. We suspect with larger patient data sets that this slope might further deviate from 1 as we expect to observe a nonlinear extraction at higher flow rates relative to the ^{13}N-NH$_3$ PET extraction [4]. The slightly higher negative bias of the ST-MLEM K_1 data compared with MLEM might be due in part to ST-MLEM overestimation of the blood pool TAC, as illustrated in **Figure 1A**, which in turn might be due to the ST-MLEM basis functions not sufficiently representing a complete set of basis functions for the SPECT data.

Although the dynamic SPECT acquisition and its ability to accurately estimate kinetic parameters such as myocardial blood flow using conventional two-headed gamma camera is our focus of the current study, we also have to note that recently introduced dedicated cardiac SPECT scanners such as D-SPECT (Spectrum Dynamics, Caesarea, Israel), Cardiac (Cardiac, Canton, MI), and Discovery NM 530 c and NM/CT 570 c (GE Healthcare, Tirat Carmel, Israel) can be used to acquire dynamic MPI data for the same parameter estimation. Since the newer technologies implemented in these dedicated cardiac SPECT systems may provide improved sensitivity and/or spatial resolution, the results obtainable from these scanners could also provide improved parameter estimation accuracy over the results reported here using the conventional technology. One important potential improvement using a newer technology that offers higher sensitivity is that we should be able to use a lower administered dose of ^{99m}Tc-based radiopharmaceuticals such as ^{99m}Tc-MIBI than currently administered amount for dynamic or conventional static SPECT MPI.

Conclusion

Myocardial to blood pool contrast measurements indicate that the ST-MLEM reconstruction shows significantly improved image quality compared to MLEM reconstruction of dynamic ^{99m}Tc-MIBI MPI rest data. Myocardial uptake coefficient estimation of K_1 with ^{99m}Tc-MIBI and ST-MLEM provided reasonable agreement with PET data (r=0.88, $p<0.17$), but we were unable to show that it was significantly better than with MLEM. A larger number of patients would be necessary to determine if the ST-MLEM is truly better than MLEM, and whether such reconstructions could be part of a quantitative SPECT protocol.

Acknowledgements

Disclosure of conflict of interest

None.

Address correspondence to: Dr. Youngho Seo, UCSF Physics Research Laboratory, Department of Radiology and Biomedical Imaging, University of California, San Francisco, CA, USA. E-mail: youngho.seo@ucsf.edu

References

[1] Bergmann SR, Herrero P, Markham J, Weinheimer CJ and Walsh MN. Noninvasive quantitation of myocardial blood flow in human subjects with oxygen-15-labeled water and positron emission tomography. J Am Coll Cardiol 1989; 14: 639-652.

[2] Muzik O, Beanlands RS, Hutchins GD, Mangner TJ, Nguyen N and Schwaiger M. Validation of nitrogen-13-ammonia tracer kinetic model for quantification of myocardial blood flow using PET. J Nucl Med 1993; 34: 83-91.

[3] El Fakhri G, Kardan A, Sitek A, Dorbala S, Abi-Hatem N, Lahoud Y, Fischman A, Coughlan M, Yasuda T and Di Carli MF. Reproducibility and accuracy of quantitative myocardial blood flow assessment with (82)Rb PET: comparison with (13)N-ammonia PET. J Nucl Med 2009; 50: 1062-1071.

[4] Saraste A, Kajander S, Han C, Nesterov SV and Knuuti J. PET: Is myocardial flow quantification a clinical reality? J Nucl Cardiol 2012; 19: 1044-1059.

[5] Gullberg GT, Reutter BW, Sitek A, Maltz J and Budinger TF. Dynamic single photon emission computed tomography – Basic principles and cardiac applications. Phys Med Biol 2010; 55: R111-R191.

[6] Tsuchida T, Yonekura Y, Takahashi N, Nakano A, Lee JD, Sadato N, Yamamoto K, Waki A, Sugimoto K, Hayashi N and Ishii Y. A trial for the quantification of regional myocardial blood flow with continuous infusion of Tc-99m MIBI and dynamic SPECT. Ann Nucl Med 1999; 13: 61-64.

[7] Winant CD, Aparici CM, Zelnik YR, Reutter BW, Sitek A, Bacharach SL and Gullberg GT. Investigation of dynamic SPECT measurements of the arterial input function in human subjects using simulation, phantom and human studies. Phys Med Biol 2012; 57: 375-393.

[8] Stowers SA and Umfrid R. Supine-prone SPECT myocardial perfusion imaging: the poor man's attenuation compensation. J Nucl Cardiol 2003; 10: 338.

[9] Hayes SW, De Lorenzo A, Hachamovitch R, Dhar SC, Hsu P, Cohen I, Friedman JD, Kang X and Berman DS. Prognostic implications of combined prone and supine acquisitions in patients with equivocal or abnormal supine myocardial perfusion SPECT. J Nucl Med 2003; 44: 1633-1640.

[10] Malkerneker D, Brenner R, Martin WH, Sampson UK, Feurer ID, Kronenberg MW and Delbeke D. CT-based attenuation correction versus prone imaging to decrease equivocal interpretations of rest/stress Tc-99m tetrofosmin SPECT MPI. J Nucl Cardiol 2007; 14: 314-323.

[11] Reutter BW, Gullberg GT, Boutchko R, Balakrishnan K, Botvinick E and Huesman RH. Fully 4-D dynamic cardiac SPECT image reconstruction using spatiotemporal B-spline voxelization. IEEE Nuclear Science Symposium Conference Record 2007; 6: 4217-4221.

[12] Forsgren A, Gill PE and Wright MH. Interior methods for nonlinear optimization. SIAM Rev 2002; 44: 525-597.

[13] Yoshida K, Mullani N and Gould KL. Coronary flow and flow reserve by PET simplified for clinical applications using rubidium-82 or nitrogen-13-ammonia. J Nucl Med 1996; 37: 1701-1712.